1E). Congo red staining of selected cerebral and cerebellar cortices was negative.

Immunohistochemistry

PrP immunostaining with Mabs 3F4 and 1E4 of the cerebral cortex, basal ganglia, and thalamus from the PSPr cases was strong, and in the hippocampal formation was selective with strong immunoreactivity in the molecular layer of the dentate and stratum lacunosum moleculare, without pyramidal cell layer staining (Figs 2A, B). The staining pattern in the cerebrum was characterized by round, loose clusters of coarse granules quite evenly distributed over a background of smaller granules (see Fig 2C). The size of the cluster-forming granules often increased progressively toward the cluster's center, which generally contained a larger granule or a tight aggregate of small granules (see Fig 2D). Strongly immunostained globular structures were occasionally seen, rarely also in the white matter (see Fig 2D; inset). Immunoreactivity in cerebellum and brainstem was limited to minute, rounded structures or aggregates of a few granules in the cerebellar molecular layer and midbrain colliculi, except for one subject who displayed a large number of these structures (see Fig 2H). The immunostained clusters and globules could not be correlated with histologically detectable lesions except for the intense immunostaining of possible microplaques in the cerebellum of some cases (see Figs 1D and Fig 2H). The pattern of PrP immunostaining of cerebrum and cerebellum in the PSPr cases was readily distinguishable from those of sCJD subtypes and nonprion disease controls (see Figs 2E–J). Furthermore, on paraffin-embedded tissues, PrP immunoreactivity was virtually removed with PK treatment (50μg/ml, 37°C, 1 hour) in these cases, whereas it was only reduced in sCJD (data not shown). Amyloid-β immunostaining showed mostly diffuse plaques apparently compatible with the subject's age.

Electron Microscopy

The ultrastructural examination of the cerebellar molecular layer from the case shown in Figure 1D showed poorly defined, rounded structures with barely detectable filament-like profiles that were embedded in an amorphous-granular matrix. These formations strongly reacted with antibodies to PrP and overall had the features of poorly formed or immature PrP microplaques (Figs 3A, B).

Genetic Findings

All PSPr patients were homozygous for valine at codon 129 of the PrP gene, and none carried mutations in the PrP gene ORF; three subjects had silent polymorphisms (two at codon 117 and one at codon 122).

Prion Protein Characterization: Detergent-Insoluble, Protease-Resistant, and Protease-Sensitive Prion Protein

The total PrP immunoblot profile from all PSPr patients was indistinguishable from that of nonprion disease control subjects (Fig 4A). The glycoform ratios of the three PrP bands from the two groups were similar. Measured by densitometry in arbitrary units, the diglycosylated or upper band was 10.44 ± 1.78 (n = 3) in PSPr versus 7.83 ± 3.64 (n = 5) in nonprion disease control subjects ($p = 0.30$); the monoglycosylated or intermediate band was 4.40 ±1.88 (n = 3) in PSPr versus 3.40 ± 2.74 (n = 5) in control subjects ($p = 0.79$). Under our conditions, the unglycosylated or lower band was not measurable in both PSPr patients and control subjects (see Fig 4A). Furthermore, the mean amount of total PrP present in six subjects apparently did not significantly differ from that of the nonprion disease control subjects (n = 7) (1.69 ± 0.28 vs 1.57 ± 0.39; $p = 0.53$) and from that of cases with prion disease (n = 3) (1.69 ± 0.28 vs 2.03 ± 0.46; $p = 0.20$).

In conventional diagnostic immunoblot procedures using Mab 3F4, classic PrPr (PrP27-30) was undetectable in the brain homogenates from the frontal cortex of all 11 subjects, and from the occipital and cerebellar cortices of the 7 subjects in which these brain regions were tested (see Fig 4A). Treatment with various doses of PK showed no consistent difference between these subjects and nonprion disease control subjects in these brain regions (see Fig 4B). Barely detectable amounts of approximately 6kDa PK-resistant PrP (PrP~6) were present in the temporal cortex of three of the eight tested subjects. Of the eight subjects for whom subcortical regions (substantia nigra, putamen, and thalamus) were available, significant quantity of PK-resistant PrP27-30 was found in one case, and minimal amounts in two others (one showed small amounts of PrP~6 only), whereas no PrPr could be definitely detected in the other five subjects (see Fig 4C). In contrast, probing with Mab 1E4 demonstrated a ladder of PK-resistant PrP fragments ranging from approximately 29 to 6kDa in all PSPr cases examined (see Fig 4D). The ladder-like electrophoretic mobility of the PrPr fragments did not match those associated with common subtypes of CJD, except for an approximately 20kDa fragment, which, after deglycosylation, was tentatively identified as the unglycosylated form of PrPr (see Fig 4C; also data not shown).[2] The approximately 6kDa fragment was also unglycosylated and was reminiscent of the PrP~7 fragment of GSS.[1] These fragments were most obvious at PK concentrations of 5 to 10μg/ml and decreased at greater PK concentrations. The ladder-like electrophoretic profile of PrP treated with PK was highly reproducible and was observed in all 11 PSPr cases examined. In contrast, the PrPr frag-

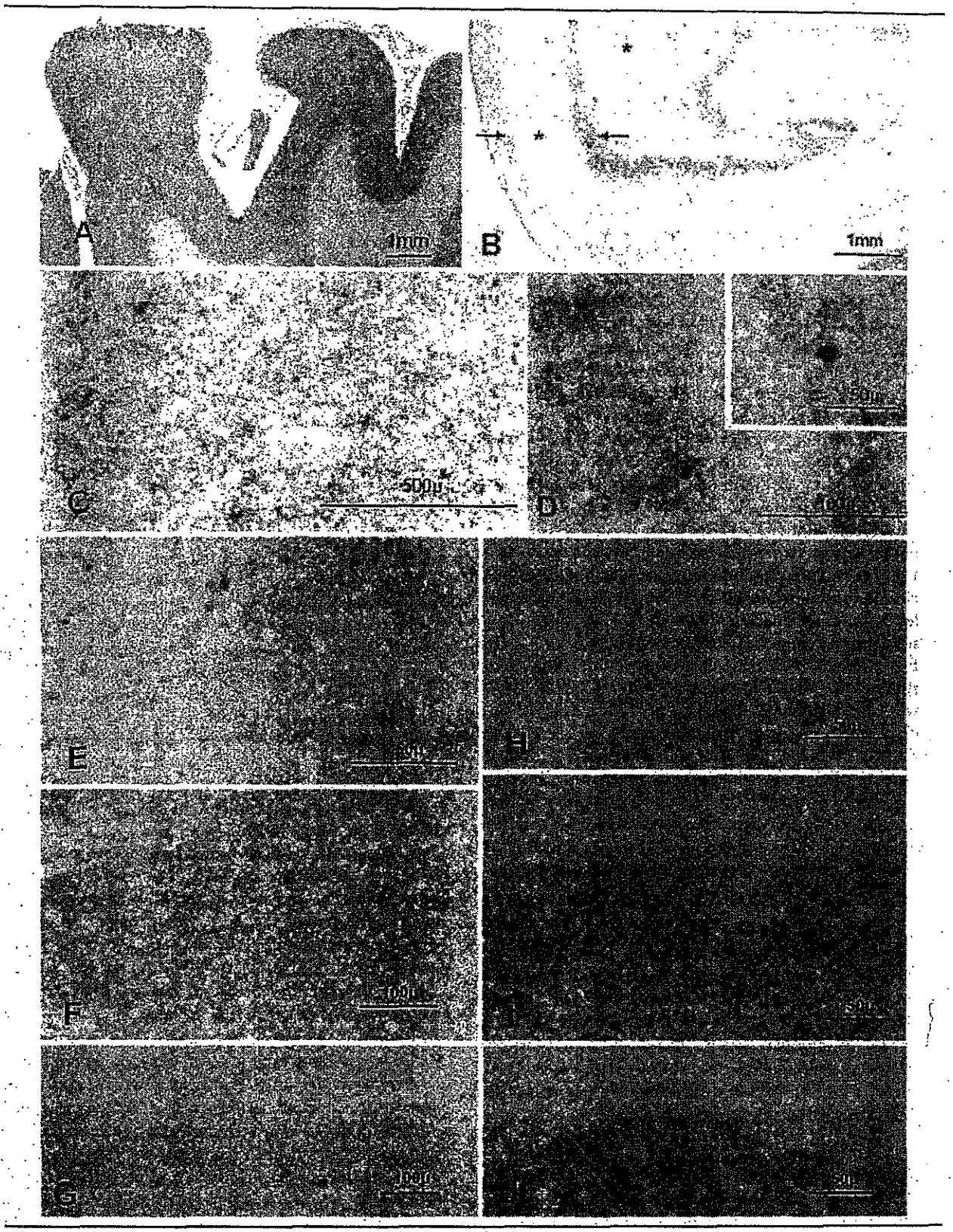

Figure 2.

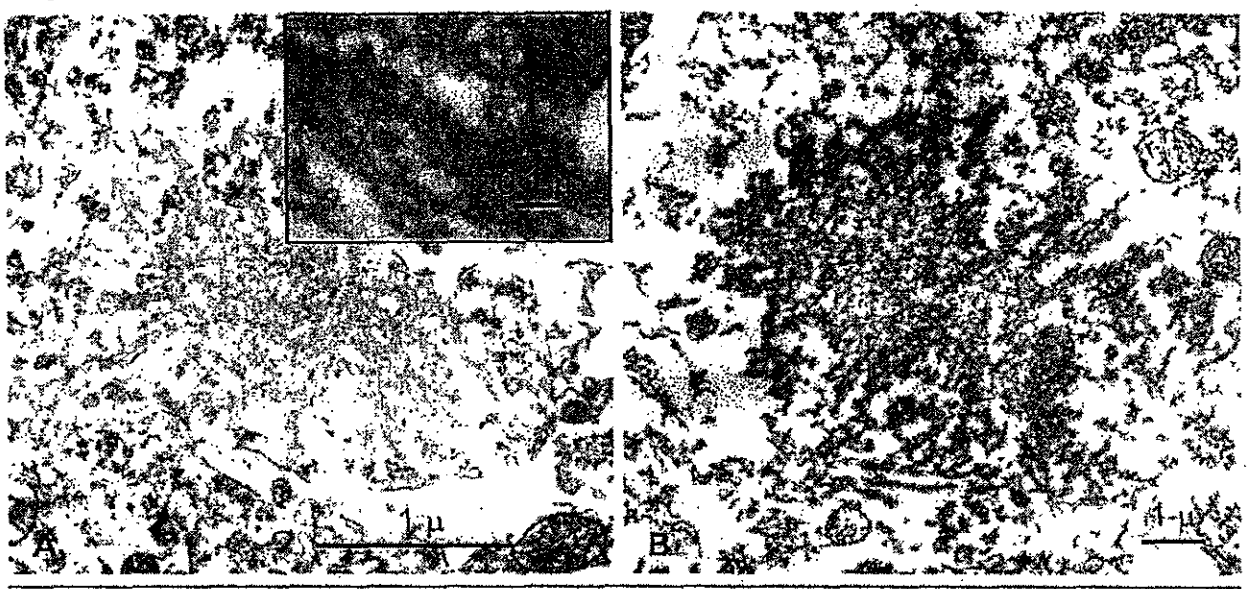

Fig 3. Electron microscopy (EM) of brain microstructures of protease-sensitive prionopathy (PSPr). (A) EM of the eosinophilic microstructures observed at light microscopy (Fig 1D) shows plaquelike formations with fuzzy filamentous appearance (inset). These structures are strongly reactive with antibodies to prion protein (PrP) (B) consistent with PrP microplaques (peroxidase anti-peroxidase with 3F4).

ments from sCJD were clearly detectable with both 3F4 and 1E4 Mab only after treatment with more than 10μg/ml PK, and increased with greater PK concentrations (see Fig 4C; also data not shown). Therefore, a small amount of PrPr detectable with Mab 3F4 is present mostly in the subcortical regions of these subjects. Moreover, most of the PrPr appears to have a different conformation from that of typical PrPr because on PK digestion it generates a unique set of fragments that are detected by 1E4 but not by 3F4.

Fig 2. Prion protein (PrP) immunohistochemistry. (A) Intense and widespread PrP immunostain of the cerebral cortex and (B) distinctive PrP immunostaining pattern in the hippocampal gyrus with staining of the molecular layers (arrows) *but not of the pyramidal cell layer or of the end plate* (asterisk). *(C, D) The cortical staining consists of coarse granules forming loose clusters with larger granules or a tighter aggregate of granules at the center; (D, inset) heavily stained globular structures are also present. (A–D) Protease-sensitive prionopathy (PSPr). (E, F) Immunostaining patterns of the cerebral cortex in sCJDVV2 (E) and sCJDVV1 (F) showing laminar staining and occasional perineuronal staining in sCJDVV2 and weak and fine widespread staining in sCJDVV1. (G) No immunostaining is detectable in the cerebral cortex of a nonprion disease control. (H–J) Cerebellar immunostaining patterns in PSPr (H), sCJDVV2 (I), and sCJDVV1 (J). There is intense and exclusive staining of large granules in the molecular layers in PSPr (H), presumably corresponding to the eosinophilic microstructures surrounded by a pale halo shown in Figure 1D; staining of irregular deposit limited to the granule cell layer in sCJDVV2 (I); no detectable staining in sCJDVV1 (the staining of the granule cell nuclei is nonspecific) (J). (A–I) Monoclonal antibody 3F4.*

Total abnormal PrP and the PrPr conformers were further characterized in abnormal PrP-enriched preparations after the capture of the abnormal PrP with g5p, a single-stranded DNA binding protein with a high affinity for abnormal PrP regardless of its PK resistance.[13,23] The amount of PrP captured by g5p in the PSPr subjects was three times greater than the amount of PrP captured in nonprion disease control subjects (data not shown), but it was nearly 16 times less than the g5p-captured PrP in typical sCJD. As measured by densitometry in arbitrary units, the mean PrP captured by g5p in eight of PSPr subjects was 3.44 ± 2.8% of the total PrP detected by direct gel loading compared with 53.55 ± 24.6% in sCJD ($n = 3$; $p = 0.00015$; Fig 5A). Furthermore, although nearly 90% of the g5p-captured PrP was resistant to PK digestion in sCJD, the PrPr accounted for only 24% of the total abnormal PrP captured in the PSPr subjects (87.59 ± 26.8% in four sCJD cases vs 24.23 ± 14.9% in nine PSPr cases; $p = 0.0001$) (see Fig 5A). The PK-resistant PrP obtained after PrP enrichment from the subjects was distributed in three major bands of approximately 26, 20, and 6kDa, which were detected by both 3F4 and 1E4, and matched the major bands of the immunoblot ladder detected with 1E4 on direct loading (see Fig 5A; also data not shown). A similar PrP banding pattern was obtained after sodium phosphotungstate precipitation, another method of abnormal PrP enrichment.[11,26] It was detected by both 3F4 and 1E4, al-